Hindawi Publishing Corporation
Journal of Chemistry
Volume 2014, Article ID 857625, 13 pages
http://dx.doi.org/10.1155/2014/857625

Research Article

Arsenic Removal from Natural Groundwater by Electrocoagulation Using Response Surface Methodology

A. M. García-Lara,[1] C. Montero-Ocampo,[2] F. Equihua-Guillen,[1] J. E. Camporredondo-Saucedo,[1] R. Servin-Castaneda,[1] and C. R. Muñiz-Valdes[3]

[1] *Facultad de Ingeniería Mecánica y Eléctrica, Universidad Autónoma de Coahuila, Avenida Barranquilla s/n, Colonia Guadalupe, C.P. 25750, 25760 Monclova, COAH, Mexico*
[2] *CINVESTAV IPN Unidad Saltillo Carretera Saltillo, Monterrey Km 13, Apdo. Postal 663, C.P. 25000, 25903 Saltillo, COAH, Mexico*
[3] *Facultad de Ingeniería, Universidad Autónoma de Coahuila, Edificio D Unidad Campo Redondo, Boulevard V. Carranza Esquina González Lobo, Colonia República Oriente, C.P. 25280, 25280 Saltillo, COAH, Mexico*

Correspondence should be addressed to A. M. García-Lara; adrianmo14@yahoo.com.mx

Received 23 September 2013; Accepted 4 May 2014; Published 23 July 2014

Academic Editor: Huu Hao Ngo

Contamination of natural groundwater by arsenic (As) is a serious problem that appears in some areas of Northern Central Mexico (NCM). In this research, As was removed from NCM wells groundwater by the electrocoagulation (EC) technique. Laboratory-scale arsenic electroremoval experiments were carried out at continuous flow rates between 0.25 and 1.00 L min^{-1} using current densities of 5, 10, and 20 A m^{-2}. Experiments were performed under galvanostatic conditions during 5 min, at constant temperature and pH. The response surface methodology (RSM) was used for the optimization of the processing variables (flow rate and current density), response modeling, and predictions. The highest arsenic removal efficiency from underground water (99%) was achieved at low flow rates (0.25 L min^{-1}) and high current densities (20 A m^{-2}). The response models developed explained 93.7% variability for As removal efficiency.

1. Introduction

Although water constitutes an essential element for human life, paradoxically, it has been associated with a large number of deaths from chronic diseases. This is because in many communities around the world, particularly in rural areas, people consume it without any previous treatment even when it contains arsenic or heavy metals, such as, lead, chromium, and cadmium [1, 2], as is classified by the World Health Organization (WHO) as a carcinogenic contaminant extremely aggressive for those who come into contact with it [3].

In spite of the diversity of treatment techniques for As-contaminated water, electrocoagulation technique has been used lately as a viable alternative to treat contaminated water [4, 5]. This electrochemical (EC) method consists of using an electric current to dissolve a sacrificial anode (usually iron or aluminum) in a contaminated aqueous medium with suspended, emulsified, or dissolved species. While generation of cations such as Fe^{2+} or Al^{3+} occurs as a result of the electrolysis effect, gases of H_2 and O_2 are also produced. Metal ions may react with OH^- ions (produced at the cathode during the formation of H_2 gas), forming insoluble hydroxides which remove contaminants from contaminated water by complexes or flocs formed due to electrostatic attraction [6, 7].

The electrocoagulation process is affected by different factors. Among the most important are the treatment time, solution pH, resistance of the aqueous solution, current density, interelectrode distance, water flow rate, and temperature [8–13]. To date, a large variety of electrochemical reactor designs have been studied [14]; however, there is no statistical analysis to evaluate systematically the simultaneous behavior of current density and volumetric flow rate in domestic reactors. This is of great importance to determine the influence of these processing parameters on the optimum

Table 1: Composition of the experimental groundwater.

Characteristics	Value
pH	7.98 ± 0.15
Conductivity (20°C)	1014 (μS cm^{-1})
As (total)	133.00 μg L^{-1}
As (V)	122.49 μg L^{-1}
As (III)	10.51 μg L^{-1}
Fe	<0.02 mg L^{-1}
SiO_2	71.62 mg L^{-1}
SO_4^{2-}	58.41 mg L^{-1}
Hg	<0.005 mg L^{-1}

treatment time needed to achieve a high As removal efficiency inside the EC reactor when treating real natural groundwater.

Based on the foregoing, the main objective of the present investigation is to study systematically the effect of the processing variables, such as current density (i) and feedwater flow rate (Q), on the total cell potential (U), EC treatment time (t), and energy consumption (E) when processing natural groundwater extracted from Mexico's Laguna Region (also known as The Comarca Lagunera), located in Torreón, Coahuila, Mexico. The response surface methodology (RSM) was used in order to develop an empirical model and investigate the optimal behavior of the reactor.

The first step in this study is focused on the optimization of the processing parameters: current density applied to the electroremoval process and feedwater supplied to the reactor for its treatment. The only design specification is to determine the minimum treatment time (response variable) at which the level of arsenic may be low enough to comply with the current safe regulations for drinking water. In a second step, an analysis of energy consumption by the electrocoagulation process based on the processing parameters mentioned above is presented.

2. Experimental Methodology

2.1. Collection of Natural Groundwater. Natural groundwater (GW) was collected from one of the wells with higher arsenic concentrations of The Comarca Lagunera. Samples were duly identified and taken to laboratory to be chemically analyzed for determining water quality. Table 1 shows the main characteristics of the collected water.

It is worth mentioning that well water sampling was carried out based on the Mexican Standard NMX-AA-008-SCFI-2011 [15]. This norm establishes a minimum volume of water to be treated of 500 mL, which must be deposited in flat-bottom container of low alkalinity glass (i.e., borosilicate glass). According to this Standard, pH of water may change rapidly as a result of chemical, physical, and biological processes and, therefore, water must be characterized without exceeding 6 h after the sample has been collected. It is noteworthy that pH of water reported in Table 1 was measured immediately after collecting the sample.

The total As concentration in collected samples and aliquots taken during and after the EC arsenic removal process was determined by inductively couple plasma (ICP) spectrometry in a Thermo-Jarrel-Iris Intrepid II XSP spectrometer. The total arsenic concentration was 133 μg L^{-1} from which 7.90% resulted as As (III) and 92.10% as Ar (V). For high-accuracy quantification of residual arsenic in the filtered liquid samples, a standard solution of As from National Institute of Standards and Technology (NIST) was used for calibration of the IPC equipment [16].

The chemical analysis of groundwater (Table 1) gives evidence that the collected water also contains other ions like Si and SO_4^- as well as very low concentrations of Fe and Hg ions. Sulfate and mercury ions were quantified by ICP, while Si was determined by atomic absorption spectrometry (AAS) in a Thermo-Elemental AAS-Solar S4 spectrometer [17].

The residual iron (Fe) content resulting from the anodic dissolution of the electrode and contained in the aliquots taken during and after the EC arsenic removal was also monitored by AAS. Before being analyzed, each sample was filtered with cellulose filter paper of 0.45 μm pore size.

2.2. Implementation and Experimental Conditions Used for the EC Process. Arsenic electroremoval experiments were performed in an electrochemical perfectly mixing reactor. Four electrodes, 15.24 cm long × 15.24 cm wide × 0.64 cm thick, with an effective contact area of 929.03 cm^2 were used for the reactor mounting. For this EC system, the interelectrode distance was 2 mm and the volume of water to be treated in the reactor was 1.68 L. The As-contaminated feedwater was fed to the reactor from the bottom, while the resulting treated water was drained out at the upper part of it. This is in order to not only increase the contact time between the contaminated water and working electrodes but also promote higher levels of flow turbulence.

A very important factor to consider in the electrocoagulation process is the mass transfer of the electrode material generated inside the reactor, since it allows the solution residence time to decrease and the removal efficiency to be increased with lower energy consumption [18]. To intensify the movement of the liquid, a continuous air flow was injected through the bottom of the reactor at rate of 1.6 L min^{-1}. Air injection was carried out using two bubble diffusers that were connected to an ELITE800 pump. In this way, bubbles of 2 mm diameter were distributed uniformly through interelectrode spaces producing a uniform distribution of electrode metallic species produced inside the electrochemical reactor.

During experiments in the perfectly mixing reactor, the liquid flow rate was varied at 0.25, 0.5, and 1.0 L min^{-1} using a Fisher-FH100C variable-speed peristaltic pump. In addition, the applied current densities were 5, 10, and 20 A m^{-2}. Arsenic removal was carried out under galvanostatic conditions (at constant current density) using a BK precision XLN3640-GL programmable power supply, while the cell total voltage was monitored with a Steren-MUL600 professional digital multimeter with PC interface.

Water samples to be analyzed for determination of residual As concentration were collected at the exit of the reactor after 0.08, 0.17, 0.25, 0.33, 0.5, 0.75, 1, 1.5, 2, 2.5, 3, 4, and 5 min.

The response variables of electrolysis treatments were the treatment time (t), energy consumption (E), and electrode wear; the latter was expressed in terms of the amount of the electrode material dissolved during the EC process.

In situ measurements of pH were performed before and after the EC treatment. Changes in pH and conductivity were evaluated by using a STARA3295 multiparameter. In the sample analyzed right after being extracted, the obtained pH was 7.98 ± 0.15; this parameter varied slightly during the process being 7.99 and 8.35, prior and after the EC process, respectively.

In contrast, conductivity at 20°C did not show any variation neither before nor after the EC process resulting in 1548.52 μS cm^{-1}.

The addition of electrolytes, especially sodium, promotes low energy consumption. Due to this, 1 g L^{-1} sodium chloride (NaCl) was added to water to be treated prior to performing the EC experiments [6, 19]; after adding this compound, conductivity increased up to 1931.62 μS cm^{-1}.

2.3. Response Surface Analysis of the Variables U, t, and E. The potential drop (U), the treatment time (t) (needed to obtain the maximum permissible level of As in drinking water), and energy consumption (E) depend on various factors, such as the solution conductivity, net current provided to the process, interelectrode distance, and contaminated feedwater flow rate [20–22].

To analyze statistically the EC process, a factorial design that consists of two factors and three levels for each factor was used; it resulted in nine experimental treatments which allow estimation of the main effects and their interactions.

In order to avoid confusions regarding the effect of each factor and the introduction of bias into the evaluation of the treatment effects, experiments were carried out randomly [23].

It was decided to use an experimental 3 k factorial design in order to obtain considerable experimental observations and prevent laborious experimental measurements as in the 4-level factorial design or in those with more than 4 levels.

It was required that the selected design contributed to explain the issue of curvature in the response function since it implies a parabolic approach, which differs from the 2 k factorial, and, for this reason, the latter was not considered to be a good choice [24, 25]. Furthermore, the 3 k factorial design is useful to investigate quadratic effects which are of interest in the present research [26]. It is worth mentioning that the interaction taken into account for the analysis of variance presented in this work was the one between Q and i.

3. Results and Discussion

3.1. Kinetics of As Electroremoval. Figure 1 shows the residual As concentration as a function of the EC treatment time, for electrolysis experiments performed at a feedwater flow of 0.25 L min^{-1} and current densities of 5, 10, and 20 A m^{-2}. It can be seen that As is most effectively removed at a higher current density supplied to the EC process. Nevertheless, for a given current density, the concentration of As decreases

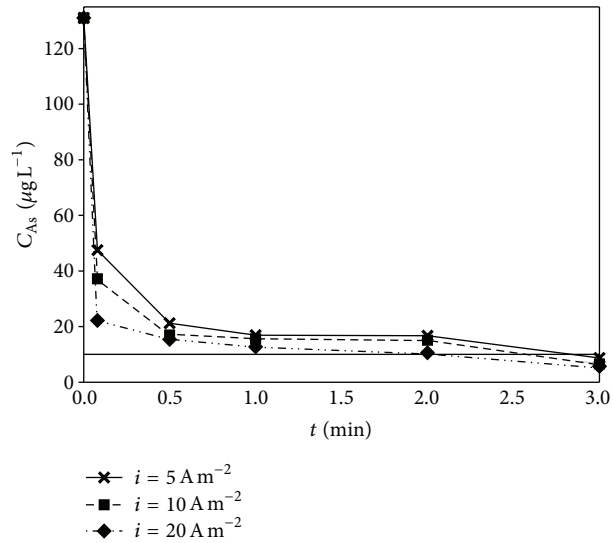

Figure 1: Kinetics of total As removal in the EC reactor for experiments carried out at a flow rate of 0.25 L min^{-1} and current densities of 5, 10, and 20 A m^{-2}.

significantly during the first 5 s of treatment, showing a reduction of 65% (47 μg L^{-1}), 72% (37 μg L^{-1}), and 83% (22 μg L^{-1}) for current densities of 5, 10, and 20 A m^{-2}, respectively. The As concentration decreases continuously as a function of the processing time, reaching the maximum permissible level in drinking water (10 μg L^{-1}) after 2.84, 2.60, and 2.12 min when applying current densities of 5, 10, and 20 A m^{-2}, respectively. The fast As removal observed at the beginning of the EC process is attributed to the fact that ions of arsenic species are abundant when electrolysis starts. Furthermore, iron hydroxides generated by the anodic electrodissolution form time-dependent complexes which are dragged by action of the applied feedwater flow out of the reactor. This behavior is consistent with the previous recent works reported by Kumar et al. [10] and Vasudevan et al. [27].

It is observed in Figure 2 that when the natural feedwater flow is increased from 0.25 to 0.50 L min^{-1}, even though adsorption kinetics is very similar, the treatment time required to reach an As concentration of 10 μg L^{-1} is slightly prolonged. For current densities of 5, 10, and 20 A m^{-2}, the treatment time needed to obtain the maximum permissible limit of As in drinking water is 2.96, 2.61, and 2.33 min, respectively.

This behavior is related to the fact that, by increasing the feedwater flow rate, the retention time of FeOOH species generated decreases resulting in an increase of the free As ions concentration in solution, due to the fact that Fe-As complexes will be formed at a lower rate.

Figure 3 shows the variations of residual As concentrations as function of treatment time for electrocoagulation experiments carried out at a liquid flow rate of 1.00 L min^{-1} and current densities of 5, 10, and 20 A m^{-2}. It can be seen that the rate at which Ar is removed is relatively fast during the first 5 s of the EC treatment; however, these

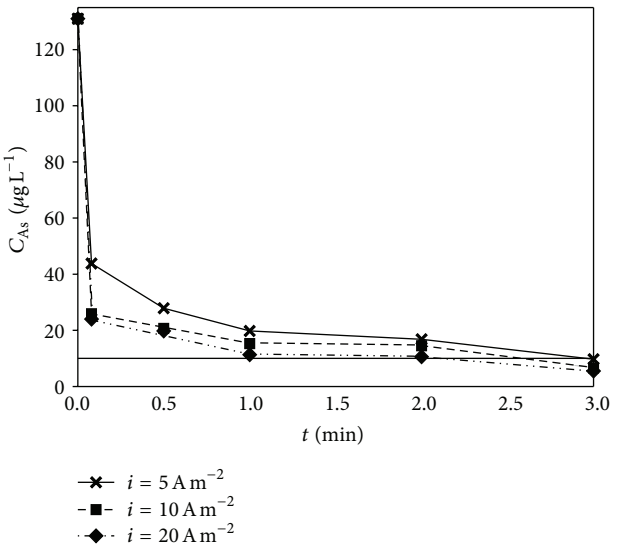

Figure 2: Variation of total As concentration in the reactor during the EC process using a feedwater flow rate of 0.50 L min^{-1} and current densities of 5, 10, and 20 A m^{-2}.

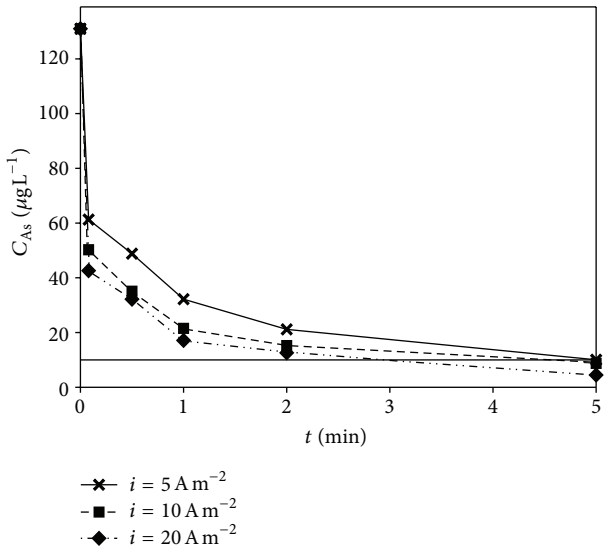

Figure 3: Kinetics of total As removal for treatments with a continuous flow of 1.00 L min^{-1} and current densities of 5, 10, and 20 A m^{-2}.

arsenic concentrations are higher than those obtained when using flow rates of 0.50 L min^{-1} or 0.25 L min^{-1}; these are 42.61 μg L^{-1} and 61.28 μg L^{-1} for applied current densities of 20 and 5 A m^{-2}, respectively.

For this flowing condition (1.00 L min^{-1}), the treatment time required to achieve an As concentration of 10 μg L^{-1} increases significantly compared to that observed with flow rates of 0.25 and 0.50 L min^{-1}. These results show that the maximum permissible As concentration established by the World Health Organization (WHO) can be obtained using current densities of 5, 10, and 20 A m^{-2} and processing times of 5.00, 4.41, and 2.95 min, respectively. As the flow rate of water to reactor increases, the contact time between As and Fe species is reduced so the rate of complex formation decreases. Therefore, a longer time is needed to ensure that iron concentration and the formation of these complexes increases.

3.2. Total Cell Potential (U) during the EC Process. The total cell potential (U) represents the sum of individual potential differences involved in the process, such as the thermodynamic potential (E_{rn}), anode overpotential (η_a), cathode overpotential (η_c), potential drop due to the electrolyte resistance (RI), and electrodes resistance (RI_E) [28–30]:

$$U = E_{rn} + \eta_a + \eta_c + RI + RI_E. \quad (1)$$

The variation of total potential measured in the electrolyzer as a function of treatment time is shown in Figure 4, for electroremoval experiments performed at current densities of 5, 10, and 20 A m^{-2} using groundwater flow rates of 0.25, 0.50, and 1.00 L min^{-1}. As can be observed in this figure, the potential drop measured at the terminals of the reactor increases significantly, when the current density is increased and the flow rate is kept constant. Important to notice is that, for the two highest current densities of 10 and 20 A m^{-2}, the cell potential decreases during the first 30 s of treatment down to an approximately constant value. This behavior is observed independently of the flow rate used. However, when a current density of 5 A m^{-2} is used, the cell potential first increases during the first 60 s of treatment up to it reaches a stable potential.

The total potentials measured at the beginning of the process using a liquid flow rate of 0.25 L min^{-1} are 2.33, 3.88, and 4.38 V, for current densities of 5, 10, and 20 A m^{-2}, respectively (Figure 4(a)). By increasing the feedwater flow rate twice, the total potentials measured in the reactor result in 1.96, 3.76, and 4.69 V with current densities of 5, 10, and 20 A m^{-2}, respectively (Figure 4(b)). In contrast, when the flow rate is 1.00 L min^{-1}, the potentials measured are 1.80, 3.51, and 5.02 V at 5, 10, and 20 A m^{-2}, respectively (Figure 4(c)). From these results, it can be concluded that the feedwater flow rate does not have a significant effect on the potential drop, which is in agreement with the results obtained by Gao et al. 2005, who reported that, at low flow rates, the increase of the potential is mainly related to the amount of hydrogen gas generated, which in turn increases as the current density is increased [31].

3.3. Determination of Residual Fe Concentration in Water Treated during the EC Process. By way of example, Figure 5 illustrates the residual Fe concentration as a function of EC treatment time for experiments carried out using a flow rate of 0.25 L min^{-1} and current densities of 5, 10, and 20 A m^{-2}. The horizontal dotted line in this figure indicates the maximum permissible concentration of Fe in drinking water, 300 μg L^{-1}, established by the WHO [32]. It was decided to measure the residual Fe analysis in experiments performed

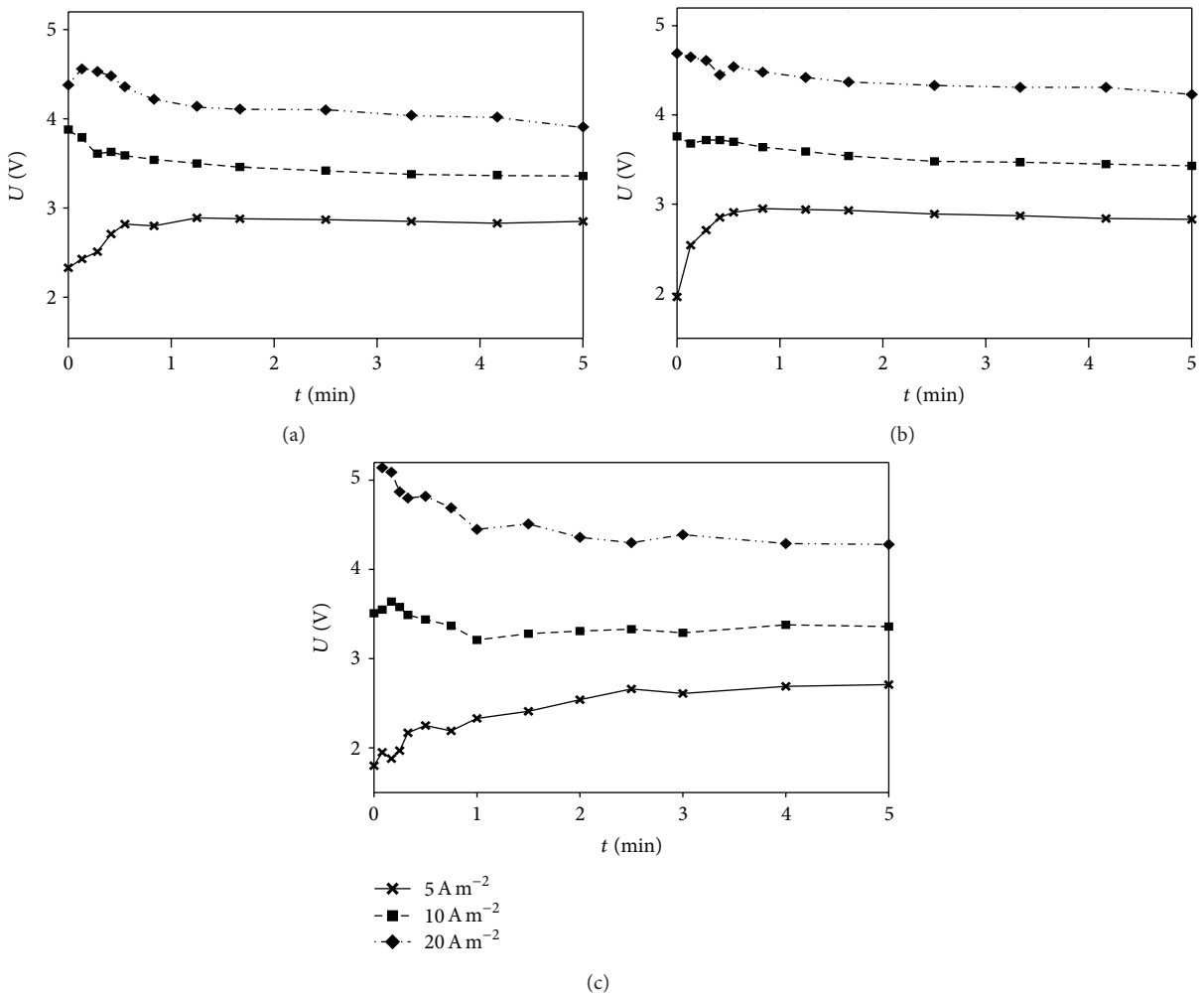

Figure 4: Variation of the potential drop as a function of the EC treatment time during As removal from natural water at different current densities (5–20 A m^{-2}) and the feedwater flow rates (a) 0.25, (b) 0.50, and (c) 1.00 L min^{-1}.

at a low flow rate, this decision was made considering the higher concentration of the electrode material generated inside the reactor during the EC process, since the residence time is maximum. According to Figure 5, the residual Fe concentration is inferior to the maximum permissible level established by the WHO (300 $\mu g\,L^{-1}$) [32]. As can be seen in this figure the Fe concentration increases as the current is increased. This behavior is attributed to the fact that generation of metal ions depends directly on the current density applied to the electrolysis. Thus, when higher current densities are used, the dosage of Fe^{2+} ions to the process is higher.

3.4. Dosing of Fe during the As Electroremoval Process. The amount of Fe released in the solution was calculated theoretically by Faraday's law (2), which is a relationship between the current density i (A m^{-2}) and the amount of Fe to be delivered (w, expressed in g) [33, 34]:

$$w = \frac{iAtM}{zF}, \tag{2}$$

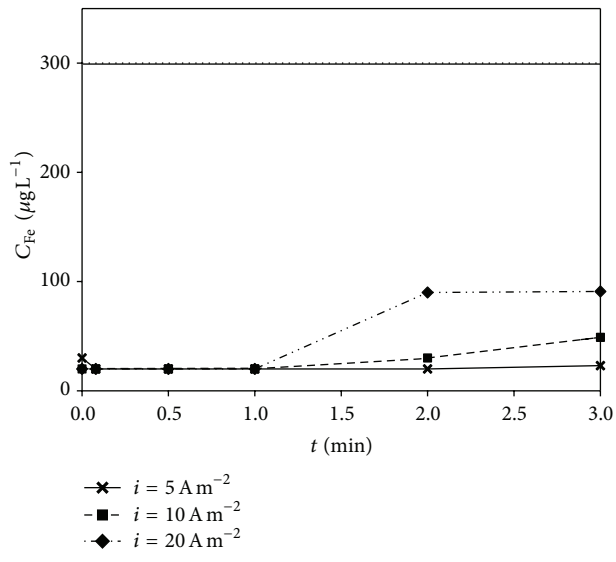

Figure 5: Variation of residual Fe concentration as a function of time for treatments carried out with a continuous flow of 0.25 L min^{-1} and applied current densities of 5, 10, and 20 A m^{-2}.

Table 2: Consumption of electrode (w) and energy (E), mean potential drop (U), and treatment time (t) to obtain an As concentration of 10 μg L^{-1} during the EC treatments with natural water performed at liquid flow rates of 0.25, 0.50, and 1.00 L min^{-1} and applied current densities of 5, 10, and 20 A m^{-2}.

Flow (L min^{-1})	i (A m^{-2})	U (V)	t (s)	w (g m^{-3})	E (Wh m^{-3})
0.25	5	2.776	170.40	13.65	50.781
	10	3.529	156.00	24.96	108.606
	20	4.176	127.20	40.71	202.952
0.50	5	2.774	177.60	14.23	52.602
	10	3.556	156.60	25.06	109.780
	20	4.409	139.80	44.74	234.349
1.00	5	2.301	300.00	24.03	70.843
	10	3.558	264.60	42.34	180.425
	20	4.639	177.00	56.65	309.815

where A represents the electrode effective area (m^2), t is the EC treatment time (s) required to obtain an As concentration of 10 μg L^{-1}, M is the molar mass of the electrode material (55.84 g mol^{-1}), z is the valence of the dissolving metal ion ($z = 2$), and F is the Faraday constant (96, 485 C mol^{-1}).

Energy consumption (E) by the EC process was calculated from the total voltage drop in the reactor (U, V), applied current density (I, A), and treatment time (t, s), by the following equation:

$$E = IUt. \tag{3}$$

The resulting w and E obtained as a function of the feedwater flow (0.25, 0.50, and 1.00 L min^{-1}) and current densities (5, 10, and 20 A m^{-2}) are summarized in Table 2. The mean total potential drop (U) was measured at each processing condition; it is also shown in this table. According to Table 2, E varies in the ranges 50.781–202.952 Wh m^{-3}, 52.602–234.349 Wh m^{-3}, and 70.843–309.815 Wh m^{-3} and w exhibits variations in the ranges 13.65–40.71 g m^{-3}, 14.23–44.74 g m^{-3}, and 24.03–56.65 g m^{-3}, when the current density and the natural water flow rate are varied from 5 to 20 A m^{-2} and from 0.25 to 1.00 L min^{-1}, respectively. From the experimental results obtained in this study it can be concluded that the flow rate has a significant effect on the response variables w and E.

3.5. Response Surface Analysis for the Working Conditions Used in the EC Reactor. The purpose of using a statistical experimental design is to provide as much information as possible, reliable and obtained by performing the minimum number of treatments [35]. In this study, the most adequate parameters were selected: Q and i each at three levels. Table 3 shows the real and staggered variables as well as the results obtained as a function of Q and i for the conditions previously mentioned.

3.5.1. Pareto Diagram (80–20 Curves). In Figure 6, Pareto diagrams obtained through the electrolysis experimental conditions show the effects of the feedwater flow rate (0.25–1.00 L m^{-1}) and current density (5–20 A m^{-2}) on the response of U, t, and E. The response variable U is mainly influenced by the current density, while the effects of the flow rate and the interaction between Q and i are practically negligible (Figure 6(a)). For the treatment time t (Figure 6(b)), both the current density and the flow rate contribute to achieving the permissible level of As in drinking water of 10 μg L^{-1} as established by the WHO [32]. In addition, energy consumption (E) is affected, in order of importance, by the current density (i), by the flow rate, and to a lesser extent by the interaction between Q and i.

3.5.2. Main Effects Diagram. The main effects diagrams for the response variables of the electrolysis experiments carried out in the EC reactor are shown in Figure 7. It can be seen that the factor i exhibits large variations being more influential in the behavior of U. In contrast, variations of Q are much less significant and can be appreciated as a practically horizontal line. Apparently, at first instance, Q does not seem to influence the potential drop (Figure 7(a)). These results let us conclude that the lowest current density (5 A m^{-2}) is the optimum.

On the other hand, As removal treatment time is influenced mainly by Q (Figure 7(b)) and to a lesser extent by current density. The latter has also a significant effect on the EC treatment duration; as the current density increases, the processing time decreases. Additionally, it can be seen that the slope of Q is opposite to that of i, which indicates an interaction between Q and i with treatment time t. These results lead to the conclusion that the optimum parameter lowest flow rate Q of 0.25 L min^{-1}. However, variations of Q observed from 0.25 to 0.50 L min^{-1} are not very significant; therefore, the effect caused by $Q = 0.50$ L min^{-1} on the behavior of t would be very similar to that produced by $Q = 0.25$ L min^{-1}.

As can be observed in Figure 7(c), the current density (i) exhibits large variations and it is the parameter that influences the response variable of energy consumption the most. In contrast, E is less affected by the flow rate which only causes a slight increment when it is increased from 0.25 to 0.50 L min^{-1}.

3.5.3. Cross-Effects Diagrams. From the cross-effects diagrams presented in Figure 8 it can be seen that Q, which did not seem to have a significant effect on the potential drop U (Figure 7(a)), has an important effect being more significant when using 1 L min^{-1} (Figure 8(a)). On the other hand, although Figures 8(b) and 8(c) show that there is no crossing of lines, they are not parallel which indicates a possible interaction as reported elsewhere [36–38].

3.5.4. Response Surface Analysis (Surface-Contour Plot). If there is an interaction effect, both variables cannot be interpreted separately. Then, the use of a statistical analysis of variance (ANOVA) as well as contour and surface plots is convenient to represent precisely the model [4, 39, 40]. Figures 9(a) and 9(b) present the contour plot of the fitted

Table 3: Processing parameters of the 3^2 factorial design and values of response variables obtained during the EC treatments performed in the perfectly mixing reactor.

Treatments T	Variables				Responses		
	Reals		Staggered				
	Q (L min^{-1})	i (A m^{-2})	X_1	X_2	U (V)	t (s)	E (Wh m^{-3})
1	0.25	5	1	1	2.776	170.40	50.781
2		10	1	2	3.529	156.00	108.606
3		20	1	3	4.176	127.20	202.952
4	0.50	5	2	1	2.774	177.60	52.602
5		10	2	2	3.556	156.60	109.780
6		20	2	3	4.409	139.80	234.349
7	1.00	5	3	1	2.301	300.00	70.843
8		10	3	2	3.558	264.60	180.425
9		20	3	3	4.639	177.00	309.815

equation and the three-dimensional response surface plot for the response variable U.

It is observed in Figure 9(b) that the minimum potential drop is obtained at a feedwater flow rate of 1 L min^{-1} using a current density of 5 A m^{-2}. Furthermore, U increases as the applied current density and the flow rate to the EC process are increased. From these two figures it can be also observed that at constant current density and variable flow rate, the change of U is not so significant compared to that obtained at constant flow rate and increasing current density. Therefore, it can be confirmed that the applied current density is the factor that produces a greater effect on the behavior of the potential drop response variable.

The response variable t was analyzed similarly by the response surface methodology in order to evaluate the simultaneous effect of Q and i (Figures 9(c) and 9(d)). The results obtained indicate that treatment time is mostly affected by feedwater flow rate, although the effect produced by the current density on t is not negligible.

From the contour plot presented in Figure 9(c), it can be concluded that the minimum treatment time (t = 150 s) required to achieve the permissible concentration of As in drinking water, 10 μg L^{-1}, is obtained by using a current density of ~7.03 A m^{-2} and a feedwater flow rate of 0.25 L min^{-1}. By the contrary, the longest treatment time consumed during the As electroremoval experiments is observed under the following conditions: Q = 1.00 L min^{-1} and i = 5.00 A m^{-2}.

Figures 9(e) and 9(f) show the contour plot and the three-dimensional surface analysis for the response variable E. In the former, it can be noticed that the value of the response E is affected by both factors Q and i; however, the applied current density is the one that has a major influence on the change of E. For constant i and variable flow rate, the energy consumption increases slightly, but for constant volumetric flow rate and increasing current density, the response E increases considerably.

3.5.5. Empirical Model (ANOVA) for the Response Variables U, t, and E. To ensure an appropriate regression model, an analysis of variance (ANOVA) was applied and used to the formulation of a mathematical model, which takes into account both the effects of the significant variables and their respective calculated coefficients. The resulting equation (4) was used to predict the potential drop by using surface analysis (Figure 9(b)). It is worth mentioning that the experimental fit shows a certainty of 95.07% (R^2 = 0.9507), which gives evidence that the model adequately fits the data. The relationship between independent and response variables is expressed by the following polynomial equation:

$$U = 2.75 - 0.96Q + 0.07i + 0.08Qi. \quad (4)$$

The results obtained by ANOVA for the response variables U, t, and E are shown in Table 4. It can be concluded from the analysis of variance for U that the interaction between the feedwater flow rate and the current density is significant since P (0.089) is higher than α (0.05). In addition, factors Q and i also affect significantly the potential drop since P (0.001) is lower than 0.05, which indicates that these factors are significant to U. The feedwater flow rate Q has a negative effect on U; therefore, the potential drop decreases as Q is increased.

Table 4 shows the results obtained by ANOVA for the response surface t (Figure 9(d)). According to the results of this study, it is corroborated that there exists significance of the interaction Q-i ($P > 0.05$), and for the model (individual effects) the effect is significant due to the fact that the value of P is much lower (P = 0.001) than the fixed value of α. Equation (5) represents the three-dimensional surface Q-i-t presented in Figure 9(d) and shows a relatively adequate fit; the coefficient of determination (R^2) is 0.9376:

$$t = 105.90 + 226.80Q + 0.06i - 7.85Qi. \quad (5)$$

The fact that R^2 has not been close to 1 is attributed to the curvature presented in both the contour plot and the surface analysis as shown in Figures 9(c) and 9(d), respectively. This indicates, at first instance, that the quadratic model should represent in a more accurate way the behavior of the response t [41, 42].

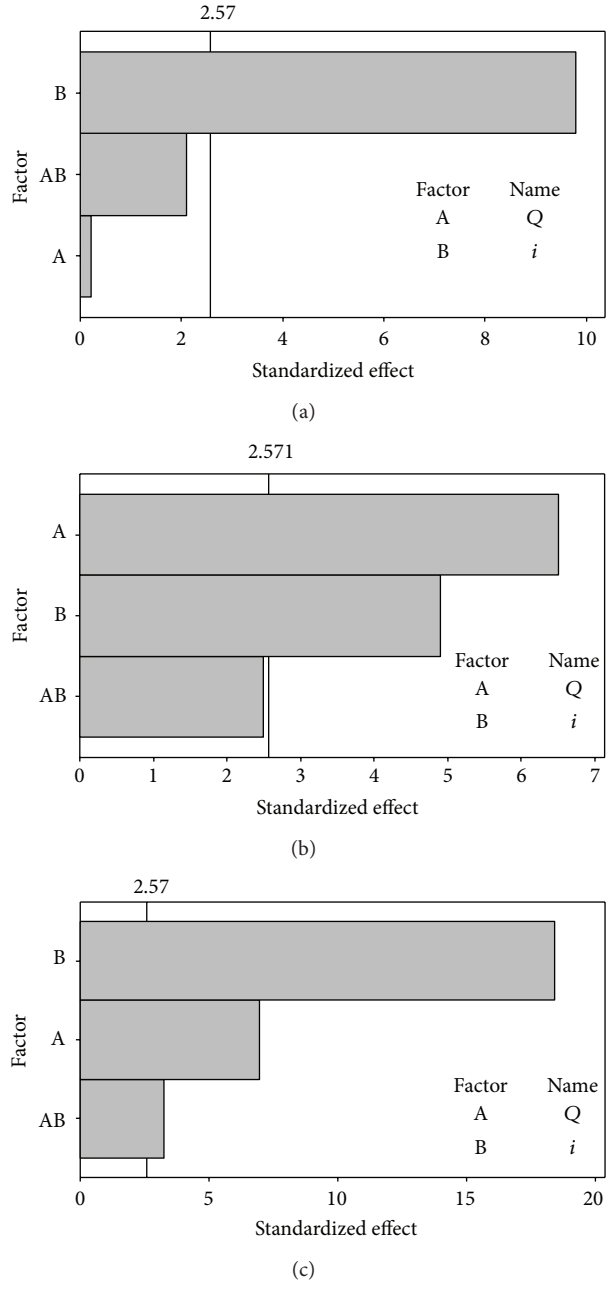

Figure 6: Pareto diagrams of effects for the response: (a) U, (b) t, and (c) E, with a 95% confidence interval ($\alpha = 0.05$).

According to the results of the analysis of variance enlisted in Table 4 for E, it is confirmed that the individual effects of Q and i ($P < \alpha$) are more significant than those produced by their interaction ($P < 0.05$). Nevertheless, these effects must be included in the mathematical model used to estimate the energy consumption by the EC process. Equation (6) presents the mathematical model described above, which has been obtained from the analysis of variance reported in Table 4. From the coefficient of determination, the fit to experimental data results in a 98.71% confidence level, which lets us confirm that such equation describes adequately the three-dimensional surface plot (Figure 9(f)) for the response of energy consumption:

$$E = -4.31 + 7.43Q + 8.37i + 7.19Qi. \quad (6)$$

4. Conclusions

The treatment time (t) needed to reach the maximum permissible level of As (10 μg L^{-1}) in experiments carried out

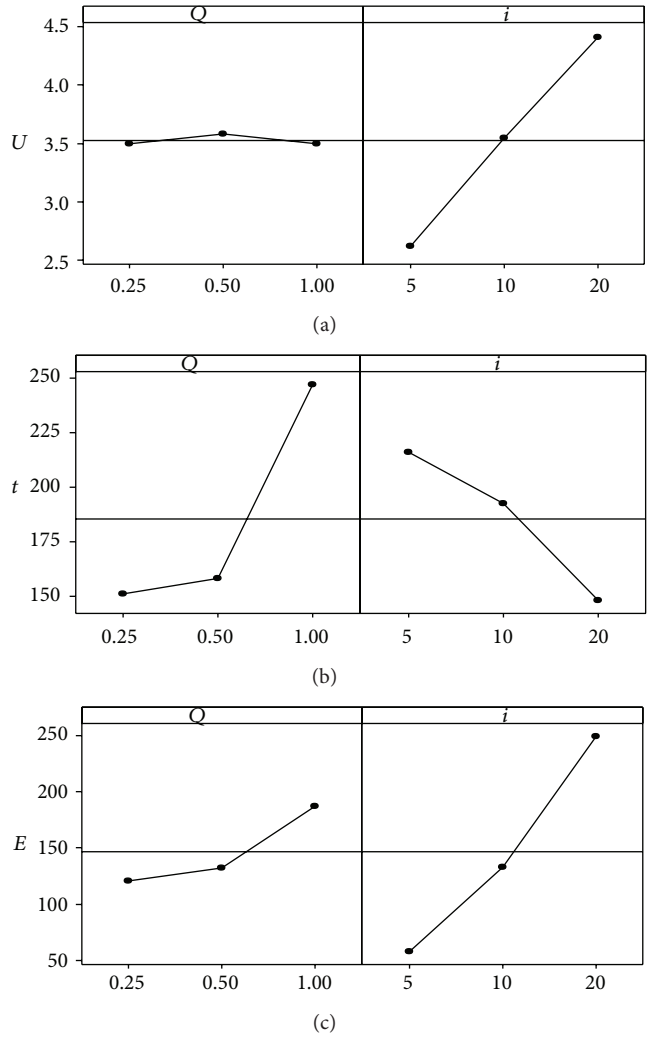

Figure 7: Main effects diagrams of feedwater flow rates Q (0.25, 0.50, and 1.00 L min^{-1}) and current densities i (5, 10, and 20 A m^{-2}) for As electroremoval treatments performed in the EC reactor on the response of (a) U, (b) t, and (c) E.

Table 4: Analysis of variance (ANOVA) for the variables investigated during the As electroremoval process, fitted to a quadratic model.

Response variable	Source of variation	Sum of squares	Degrees of freedom	Mean squares	F	P
U	Model (Q, i)	4.600	2	2.394	47.86	0.001
	Residual	0.250	5	0.050		
	Interaction	0.222	1	0.212	4.44	0.089
	Total	**5.072**	**8**			
t	Model (Q, i)	23145.000	2	11345.80	33.76	0.001
	Residual	1680.000	5	336.00		
	Interaction	2098.000	1	2097.60	6.24	0.055
	Total	**26923.000**	**8**			
E	Model (Q, i)	62612.700	2	32186.70	191.63	0.000
	Residual	839.800	5	168.00		
	Interaction	1761.400	1	1761.40	10.49	0.023
	Total	**65213.900**	**8**			

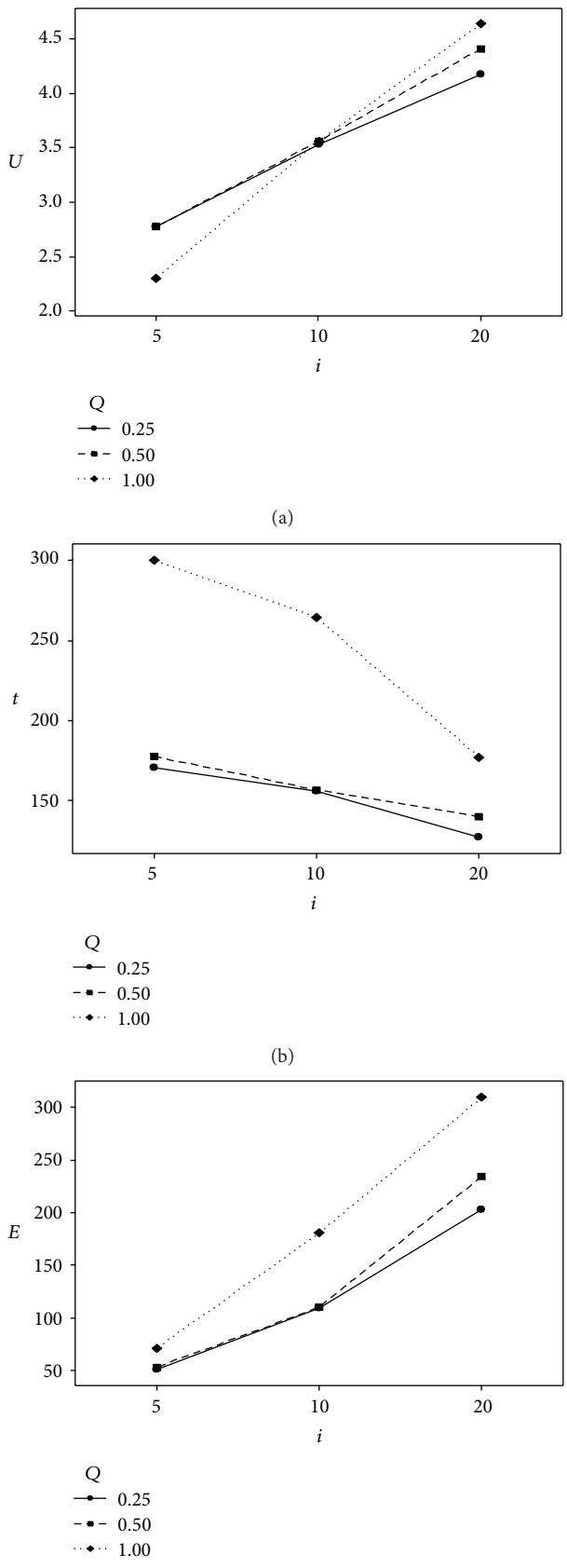

Figure 8: Cross-effects diagrams of Q and i for (a) U, (b) t, and (c) E. Experiments performed in the EC reactor applying current densities i of 5, 10, and 20 A m^{-2} and flow rates Q of 0.25, 0.50, and 1.00 L min^{-1}.

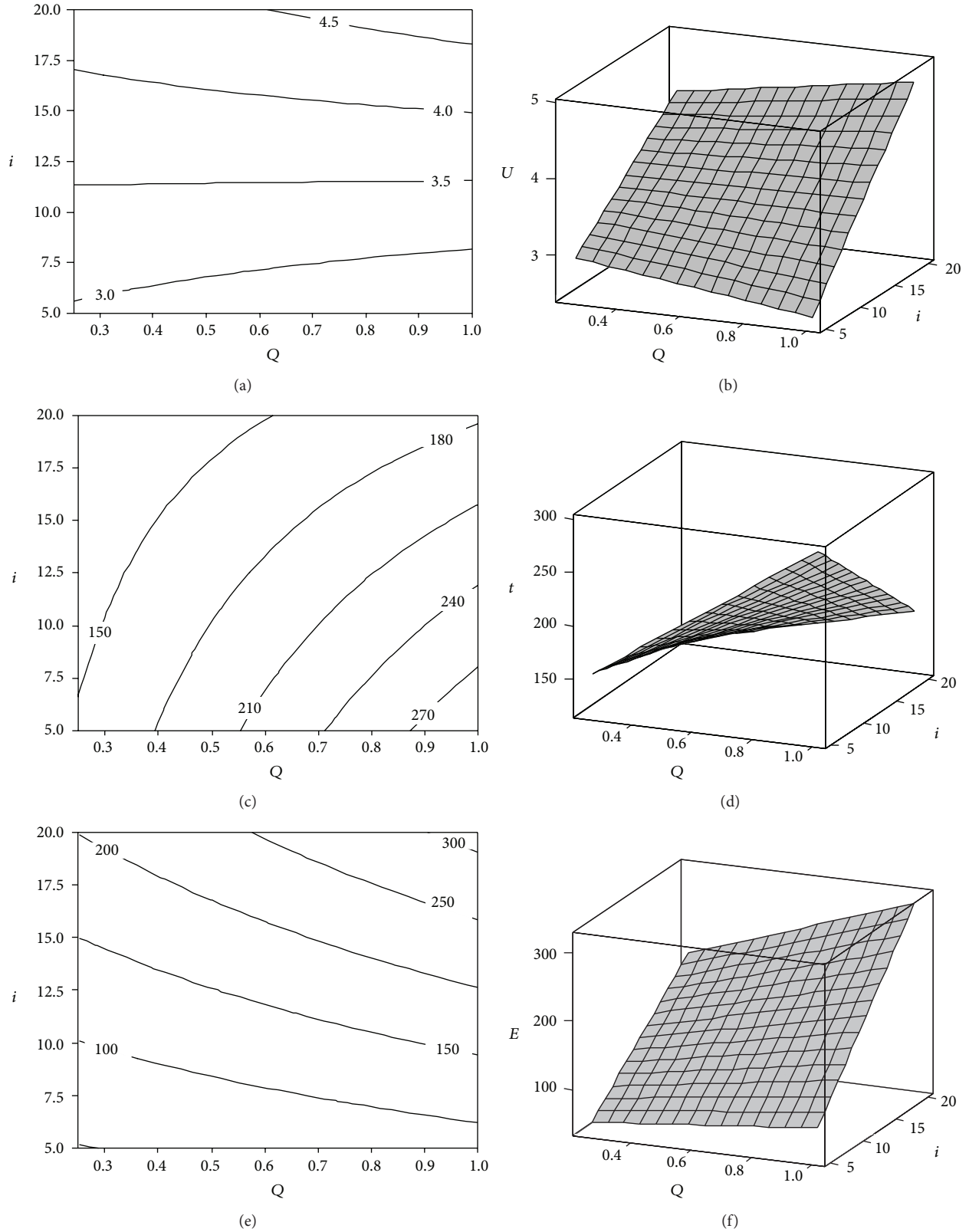

FIGURE 9: (a) Contour surface plot and (b) response surface, showing the interactive effect of feedwater flow rate Q (0.25–1.00 L min^{-1}) and current density i (5–20 A m^{-2}) on the total potential drop U measured in the EC reactor. (c) Contour surface plot and (d) response surface, showing the interactive effect between the independent variables, feedwater flow rate Q (0.25–1.00 L min^{-1}), and current density i (5–20 A m^{-2}) on the treatment time t required to achieve an As concentration of 10 μg L^{-1} during the EC process. (e) Surface contour plot and (f) surface response, showing the interactive effect of the independent variables, feedwater flow rate Q (0.25–1.00 L min^{-1}), and current density i (5–20 A m^{-2}) on energy consumption E during the EC process.

in the perfectly mixing reactor is directly proportional to the flow rate used; this is related to the fact that the contact time between As and Fe species either increases or decreases as the feedwater flow rate is decreased or increased, respectively.

The potential drop (U) measured at the terminals of the reactor for the experiments performed in the electrolyzer decreases slightly as the volumetric flow rate is increased. In contrast, it increases with higher current density and constant flow rate.

Energy consumption (E) by the EC process with groundwater varies in the range 50.781–309.815 Wh m^{-3} when the current density is increased from 5 to 20 A m^{-2} and the feedwater flow rate is varied between 0.25 and 1.00 L min^{-1}, respectively.

Pareto diagrams of effects obtained from the results of the electrolysis experiments give evidence that the response of U, t, and E is affected mainly by individual factors Q and i. However, even though the interaction Q-i has a small effect on the responses of the EC treatment, the latter cannot be arbitrarily excluded from the statistical analysis.

From the main effects diagrams of processing responses of electrolysis experiments performed in the reactor, it is observed that the lowest current density i (5 A m^{-2}) results in the lowest potential drop and energy consumption. On the other hand, it is confirmed that there exists a significant effect of the interaction Q-i on the treatment time t.

The cross-effects diagrams show that, for t and E, the interaction Q-i cannot be neglected. To support this fact, both statistical (ANOVA) and response surface analyses were performed.

According to the regression model obtained to predict the value of the response variables, the resulting polynomial equations are $U = 2.75 - 0.96Q + 0.07i + 0.08Qi$, $t = 105.90 + 226.80Q + 0.06i - 7.85Qi$, and $E = -4.31 + 7.43Q + 8.37i + 7.19Qi$. The coefficient of determination R^2 corresponding to the models obtained for U, t, and E is 0.9507, 0.9376, and 0.9871, respectively.

Results obtained by ANOVA for the response variables show that, in the case of U, the effect caused by the interaction between Q and i is significant considering that $P = 0.089$ is higher than $\alpha = 0.05$. For the response variable t there exists statistical significance in both the interaction Q-i ($P > 0.05$) and the model (individual effects) since P is much lower ($P = 0.001$) than the fixed value of α. While the individual effects of Q and i ($P < \alpha$) are significant in the behavior of E, the effects caused by their interaction are not so significant ($P < 0.05$).

From the contour plot for t, it can be concluded that the minimum treatment time ($t = 150$ s) required to reach an As concentration of 10 μg L^{-1} can be achieved by using a current density of ~7.03 A m^{-2} and a feedwater flow rate of 0.25 L min^{-1}.

Conflict of Interests

The authors declare that there is no conflict of interests regarding the publication of this paper.

Acknowledgments

The authors of this research would like to extend a special acknowledgement to CONACyT (38467U) and SEP-PROMEP (UACOAH-PTC-216) for the financial support to carry out this project.

References

[1] M. Mizanur Rahman Sarker, "Determinants of arsenicosis patients'perception and social implications of arsenic poisoning through groundwater in Bangladesh," *International Journal of Environmental Research and Public Health*, vol. 7, no. 10, pp. 3644–3656, 2010.

[2] J. Qiao, Z. Jiang, B. Sun, Y. Sun, Q. Wang, and X. Guan, "Arsenate and arsenite removal by $FeCl_3$: effects of pH, As/Fe ratio, initial As concentration and co-existing solutes," *Separation and Purification Technology*, vol. 92, pp. 106–114, 2012.

[3] E. Lacasa, P. Cañizares, C. Sáez, F. J. Fernández, and M. A. Rodrigo, "Removal of arsenic by iron and aluminium electrochemically assisted coagulation," *Separation and Purification Technology*, vol. 79, pp. 15–19, 2011.

[4] J. F. Martínez-Villafañe and C. Montero-Ocampo, "Optimisation of energy consumption in arsenic electro-removal from groundwater by the Taguchi method," *Separation and Purification Technology*, vol. 70, no. 3, pp. 302–305, 2010.

[5] A. M. García-Lara and C. Montero-Ocampo, "Improvement of arsenic electro-removal from underground water by lowering the interference of other ions," *Water, Air, and Soil Pollution*, vol. 205, no. 1–4, pp. 237–244, 2010.

[6] G. Chen, "Electrochemical technologies in wastewater treatment," *Separation and Purification Technology*, vol. 38, no. 1, pp. 11–41, 2004.

[7] P. K. Holt, G. W. Barton, and C. A. Mitchell, "The future for electrocoagulation as a localised water treatment technology," *Chemosphere*, vol. 59, no. 3, pp. 355–367, 2005.

[8] A. M. García-Lara, C. Montero-Ocampo, and F. Martínez-Villafañe, "An empirical model for treatment of arsenic contaminated underground water by electrocoagulation process employing a bipolar cell configuration with continuous flow," *Water Science and Technology*, vol. 60, no. 8, pp. 2153–2160, 2009.

[9] P. K. Holt, G. W. Barton, M. Wark, and C. A. Mitchell, "A quantitative comparison between chemical dosing and electrocoagulation," *Colloids and Surfaces A: Physicochemical and Engineering Aspects*, vol. 211, no. 2-3, pp. 233–248, 2002.

[10] P. R. Kumar, S. Chaudhari, K. C. Khilar, and S. P. Mahajan, "Removal of arsenic from water by electrocoagulation," *Chemosphere*, vol. 55, no. 9, pp. 1245–1252, 2004.

[11] I. Ali, V. K. Gupta, T. A. Khan, and M. Asim, "Removal of arsenate from aqueous solution by electro-coagulation method using Al-Fe electrodes," *International Journal of Electrochemical Science*, vol. 7, no. 3, pp. 1898–1907, 2012.

[12] M. Saleem, A. A. Bukhari, and M. N. Akram, "Electrocoagulation for the treatment of wastewater for reuse in irrigation and plantation," *Journal of Basic and Applied Sciences*, vol. 7, no. 1, pp. 11–20, 2011.

[13] K. Dermentzis, A. Christoforidis, E. Valsamidou, A. Lazaridou, and N. Kokkinos, "Removal of hexavalent chromium from electroplating wastewater by electrocoagulation with iron electrodes," *Global Nest Journal*, vol. 13, no. 4, pp. 412–418, 2011.

[14] M. Y. A. Mollah, P. Morkovsky, J. A. G. Gomes, M. Kesmez, J. Parga, and D. L. Cocke, "Fundamentals, present and future perspectives of electrocoagulation," *Journal of Hazardous Materials*, vol. 114, no. 1–3, pp. 199–210, 2004.

[15] Official Mexican Norm NMX-AA-008-SCFI-2011, "Water analysis—determination of pH—test method," Official Journal of the Federation, Mexico City, Mexico, October 2011.

[16] Official Mexican Norm NMX-AA-115-SCFI-2001, "Water analysis—general criteria for the quality—control of analitical results," Official Journal of the Federation, Mexico City, Mexico, March 2011.

[17] Official Mexican Norm NMX-AA-051-SCFI-2001, "Water analysis—determination of metals by atomic Absorption in natural, drinking, wastewaters and wastewaters treated—test method," Official Journal of the Federation, Mexico City, Mexico, September 2001.

[18] N. Vivek Narayanan and M. Ganesan, "Use of adsorption using granular activated carbon (GAC) for the enhancement of removal of chromium from synthetic wastewater by electrocoagulation," *Journal of Hazardous Materials*, vol. 161, no. 1, pp. 575–580, 2009.

[19] J. A. G. Gomes, P. Daida, M. Kesmez et al., "Arsenic removal by electrocoagulation using combined Al-Fe electrode system and characterization of products," *Journal of Hazardous Materials*, vol. 139, no. 2, pp. 220–231, 2007.

[20] A. E. Yilmaz, R. Boncukcuoğlu, M. M. Kocakerim, and B. Keskinler, "The investigation of parameters affecting boron removal by electrocoagulation method," *Journal of Hazardous Materials*, vol. 125, no. 1–3, pp. 160–165, 2005.

[21] W. Den and C.-J. Wang, "Removal of silica from brackish water by electrocoagulation pretreatment to prevent fouling of reverse osmosis membranes," *Separation and Purification Technology*, vol. 59, no. 3, pp. 318–325, 2008.

[22] C.-Y. Hu, S.-L. Lo, and W.-H. Kuan, "Simulation the kinetics of fluoride removal by electrocoagulation (EC) process using aluminum electrodes," *Journal of Hazardous Materials*, vol. 145, no. 1-2, pp. 180–185, 2007.

[23] R. Krishna Prasad, R. Ram Kumar, and S. N. Srivastava, "Design of optimum response surface experiments for electrocoagulation of distillery spent wash," *Water, Air, and Soil Pollution*, vol. 191, no. 1–4, pp. 5–13, 2008.

[24] D. C. Montgomery, *Design and Analysis of Experiments*, John Wiley & Sons, New York, NY, USA, 5th edition, 2001.

[25] M. D. Morris, "Class of three-level experimental designs for response surface modeling," *Technometrics*, vol. 42, no. 2, pp. 111–121, 2000.

[26] E. M. Monroe, R. Pan, C. M. Anderson-Cook, D. C. Montgomery, and C. M. Borror, "Sensitivity analysis of optimal designs for accelerated life testing," *Journal of Quality Technology*, vol. 42, no. 2, pp. 121–135, 2010.

[27] S. Vasudevan, G. Sozhan, S. Ravichandran, J. Jayaraj, J. Lakshmi, and S. M. Sheela, "Studies on the removal of phosphate from drinking water by electrocoagulation process," *Industrial and Engineering Chemistry Research*, vol. 47, no. 6, pp. 2018–2023, 2008.

[28] J. M. Bockris and A. K. N. Reddy, *Electrochemistry: Ionics*, Plenum Press, New York, NY, USA, 2nd edition, 1997.

[29] A. J. Bard and L. R. Faulkner, *Electrochemical Methods*, Wiley, New York, NY, USA, 2nd edition, 2000.

[30] I. Roussar, K. Micka, and A. Kimla, *Electrochemical Engineering II*, Elsevier Science, 1986.

[31] P. Gao, X. Chen, F. Shen, and G. Chen, "Removal of chromium(VI) from wastewater by combined electrocoagulation- electroflotation without a filter," *Separation and Purification Technology*, vol. 43, no. 2, pp. 117–123, 2005.

[32] WHO, *(World Health Organisation), Guidelines for Drinking-Water Quality*, vol. 1 of *Recommendatios*, WHO, Geneva, Switzerland, 3rd edition, 2004.

[33] I. Linares-Hernández, C. Barrera-Díaz, G. Roa-Morales, B. Bilyeu, and F. Ureña-Núñez, "A combined electrocoagulation-sorption process applied to mixed industrial wastewater," *Journal of Hazardous Materials*, vol. 144, no. 1-2, pp. 240–248, 2007.

[34] W. A. Pretorius, W. G. Johannes, and G. G. Lempert, "Electrolytic iron flocculant production with a bipolar electrode in series arrangement," *Water SA*, vol. 17, no. 2, pp. 133–138, 1991.

[35] M. Kobya, E. Demirbas, M. Bayramoglu, and M. T. Sensoy, "Optimization of electrocoagulation process for the treatment of metal cutting wastewaters with response surface methodology," *Water, Air, and Soil Pollution*, vol. 215, no. 1–4, pp. 399–410, 2011.

[36] E. Gengec, M. Kobya, E. Demirbas, A. Akyol, and K. Oktor, "Optimization of baker's yeast wastewater using response surface methodology by electrocoagulation," *Desalination*, vol. 286, pp. 200–209, 2012.

[37] T. K. Trinh and L. S. Kang, "Application of response surface method as an experimental design to optimize coagulation tests," *Environmental Engineering Research*, vol. 15, no. 2, pp. 063–070, 2010.

[38] D. L. Massart, B. G. M. Vandeginste, L. M. C. Muydens, S. Jong, P. J. Lewi, and J. Smeyers Verbeke, *Handbook of Chemometrics and Qualimetrics: Part A*, Elsevier, Amsterdam, The Netherlands, 1997.

[39] W. C. Lee, S. Yusof, N. S. A. Hamid, and B. S. Baharin, "Optimizing conditions for enzymatic clarification of banana juice using response surface methodology (RSM)," *Journal of Food Engineering*, vol. 73, no. 1, pp. 55–63, 2006.

[40] O. Chavalparit and M. Ongwandee, "Optimizing electrocoagulation process for the treatment of biodiesel wastewater using response surface methodology," *Journal of Environmental Sciences*, vol. 21, no. 11, pp. 1491–1496, 2009.

[41] F. R. Espinoza-Quiñones, A. N. Módenes, P. S. Theodoro et al., "Optimization of the iron electro-coagulation process of Cr, Ni, Cu, and Zn galvanization by-products by using response surface methodology," *Separation Science and Technology*, vol. 47, no. 5, pp. 688–699, 2012.

[42] D. Ghernaout, A. Mariche, B. Ghernaout, and A. Kellil, "Electromagnetic treatment-doubled electrocoagulation of humic acid in continuous mode using response surface method for its optimisation and application on two surface waters," *Desalination and Water Treatment*, vol. 22, no. 1–3, pp. 311–329, 2010.